

2 Simulation of the Operation of a GPR

Figure 1 depicts the simulation of the operation of a typical GPR. The FDTD computation domain includes the air and ground regions, an arbitrary number of buried objects with various properties, a source that simulates the transmitter (T) and a data recorder that simulates the receiver (R). The computational domain is terminated with PML ABCs. The mobile radar unit is composed of T and R. The signal received at R can be decomposed into three parts: (i) the direct (D) signal, (ii) the reflected (R) signal from the ground, and (iii) the scattered (S) signal from the buried inhomogeneities. The GPR is used to receive some information from the buried object. Therefore, the goal is to extract the S signal. However, since the D signal is usually much larger than the S signal, extracting S from the total signal becomes a nearly impossible task in some cases. In order to facilitate this task, some modifications on the radar unit will be proposed in the next section.

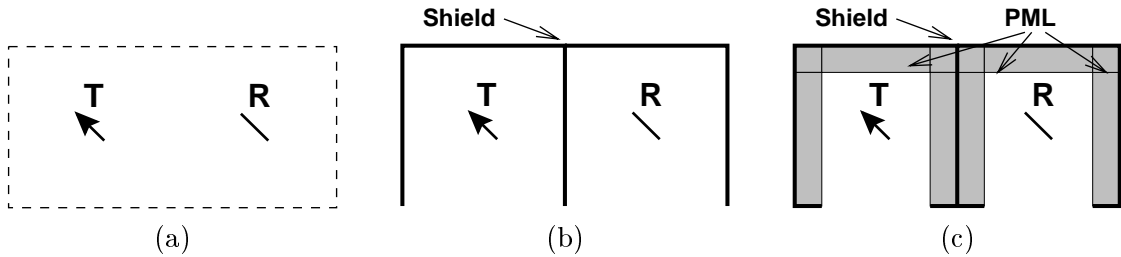


Figure 2: Three different radar units employed in the FDTD simulations.

3 Modifying the Radar Unit

Figure 2 shows three different radar units that are used in this paper: (a) T and R only, (b) T and R separated by a conducting shield, and (c) T and R separated by a conducting shield coated with PML ABCs. The shields are made up of two cubical chambers with only the bottom faces open. The shields are introduced with the intention of reducing the amplitude of the D signal so that the S signal can be extracted easily.

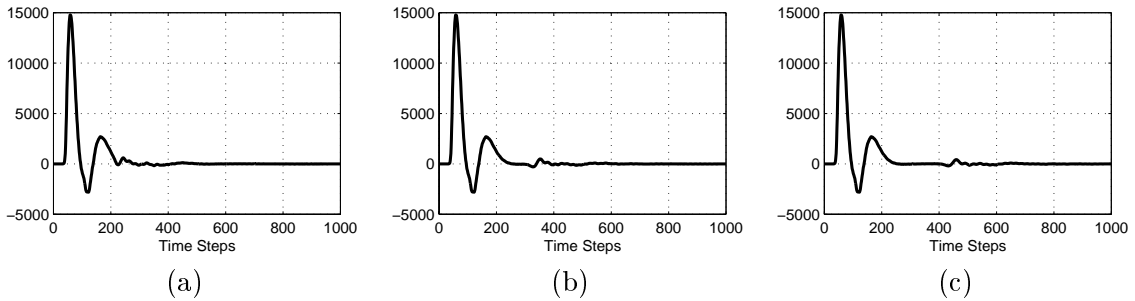


Figure 3: Total signals at the receiver when the radar unit is modeled as in Fig. 2(a) with no shield. The depth of the buried conducting box is (a) 5 cm, (b) 10 cm, (c) 15 cm.

Figure 3 shows the plots of the total signal at R when a conducting box of $5 \times 5 \times 4 \text{ cm}^3$ is buried 5, 10, and 15 cm under the ground. The ground is modeled with $\epsilon = 8$ and the center frequency of the transmitted signal is 500 MHz. The reason all three plots look

very similar is because the D signal is so large that the different T signals are almost invisible.

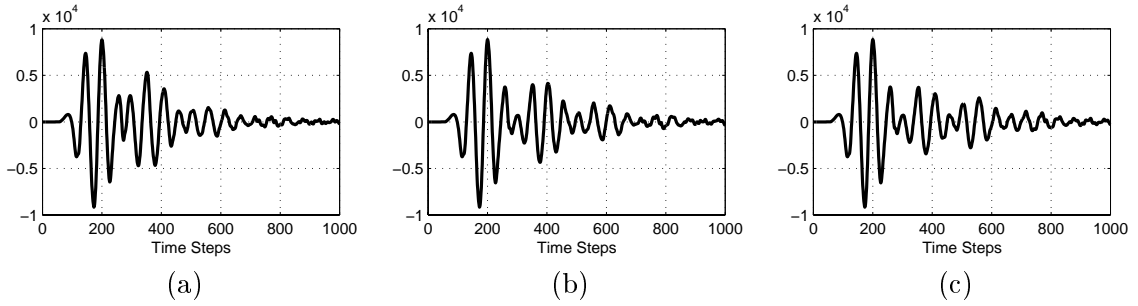


Figure 4: Total signals at the receiver when the radar unit is modeled as in Fig. 2(b) with no absorbers. The depth of the buried conducting box is (a) 5 cm, (b) 10 cm, (c) 15 cm.

Figure 4 shows the total received signals obtained with the radar configuration of Fig. 2(b). As expected, the shield reduces the amplitudes of the received signals by about 30% compared to those in Fig. 3. However, this reduction is not sufficient to allow an easy identification of the S signal in the total signal. Furthermore, the multiple reflections in the two chambers of the shield cause the signal to become oscillatory and longer in time, again hampering the detection of the S signal.

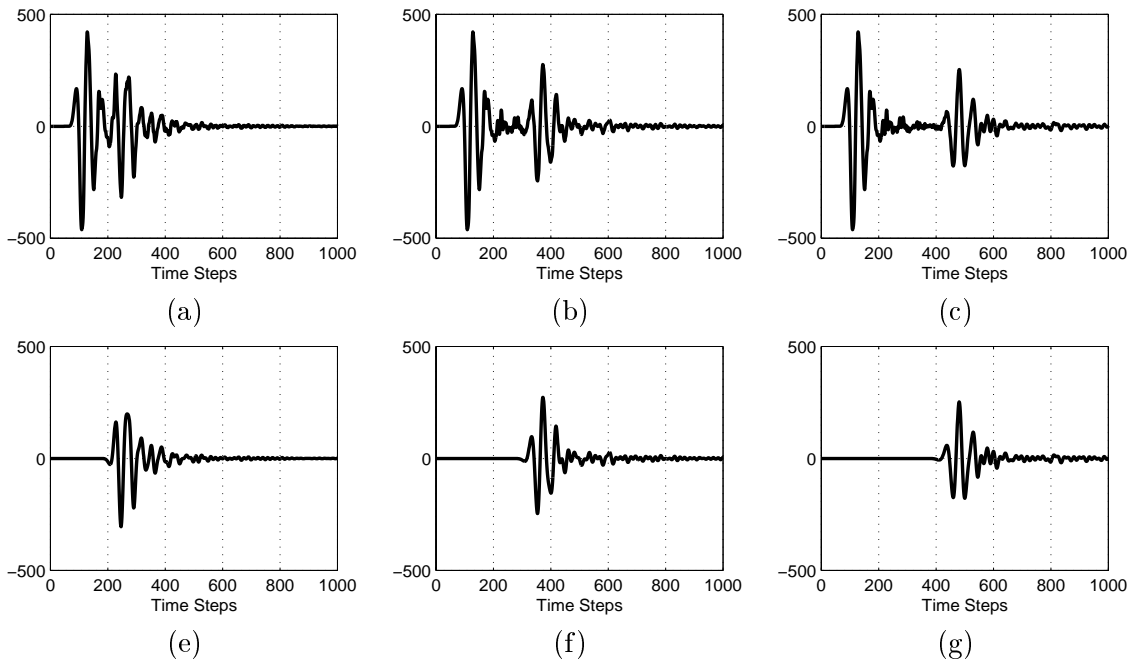


Figure 5: Total signals at the receiver when the radar unit is modeled as in Fig. 2(c) with shield and absorbers. The depth of the buried conducting box is (a) 5 cm, (b) 10 cm, (c) 15 cm. Corresponding scattered (S) signals are shown in (d), (e), and (f).

To improve the performance of the shield, we coated the interior faces of the chambers with an absorber, as shown in Fig. 2(c). For this purpose, we implemented PML ABCs

instead of modeling a material absorber. The total signals obtained at R are shown in Figs. 5(a), (b), and (c) for the three different depths of the conducting box. Note that the amplitudes of the signals are greatly reduced. In order to clearly identify the S signal in these plots, Figs. 5(d), (e), and (f) present only the S signals, which are obtained by first removing the buried object so that the receiver measures the D+R signal and then subtracting this from the total signal. Comparing Figs. 5(a), (b), and (c) to Figs. 5(d), (e), and (f), we see that S signals are easily identifiable and that the amplitudes of the D and S signals are of the same order.

Finally, Fig. 6 shows the plots of the total signals and the S signals as the radar unit of Fig. 2(c) moves over the buried objects.

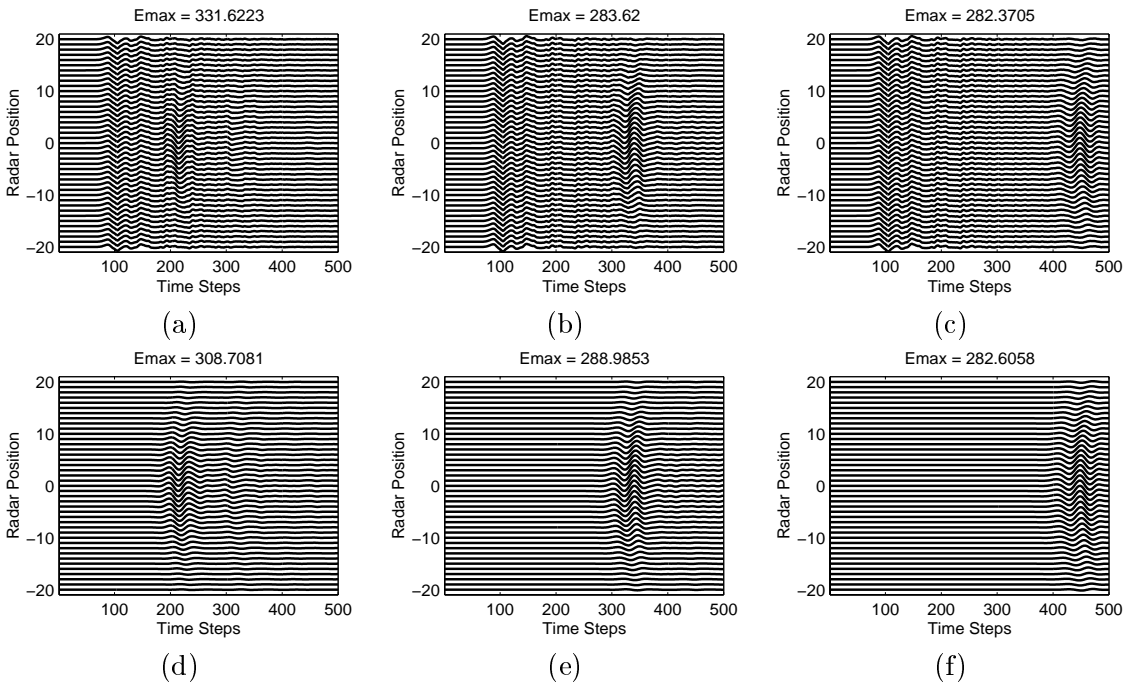


Figure 6: Total signals at the receiver when the radar unit of Fig. 2(c) moves over the ground. The depth of the buried conducting box is (a) 5 cm, (b) 10 cm, (c) 15 cm. Corresponding scattered (S) signals are shown in (d), (e), and (f).

References

- [1] K. S. Yee, "Numerical solution of initial boundary value problems involving Maxwell's equations in isotropic media," *IEEE Trans. Antennas Propagat.*, vol. AP-14, pp. 302–307, Apr. 1966.
- [2] A. Taflove, *Computational Electrodynamics: The Finite-Difference Time-Domain Method*. Boston, MA: Artech House, 1995.
- [3] K. S. Kunz and R. J. Luebbers, *The Finite Difference Time Domain Method for Electromagnetics*. Boca Raton, FL: CRC Press, 1993.
- [4] J.P. Berenger. "A perfectly matched layer for the absorption of electromagnetic waves, *J. Comput. Phys.*, pp 185-200, Oct. 1994.
- [5] U. Oğuz and L. Gürel, "Subsurface-scattering calculations via the 3D FDTD method employing PML ABC for layered media," *1997 IEEE AP-S International Symposium and URSI Radio Science Meeting*, Montréal, Canada, pp. 1920–1923, July 1997.